HHS Public Access

Author manuscript

Ann Biomed Eng. Author manuscript; available in PMC 2020 July 01.

Published in final edited form as:

Ann Biomed Eng. 2019 July ; 47(7): 1596–1610. doi:10.1007/s10439-019-02263-8.

Modeling the effect of TNF-α upon drug induced toxicity in human, tissue-engineered myobundles.

Brittany N.J. Davis[1], **Jeffrey W. Santoso**[1], **Michaela J. Walker**[1], **Catherine E. Oliver**[1], **Michael M. Cunningham**[2], **Christian A. Boehm**[3], **Danielle Dawes**[1], **Samantha L. Lasater**[1], **Kim Huffman**[4,5], **William E. Kraus**[4,5,6], and **George A. Truskey**[1]

[1]Department of Biomedical Engineering, Duke University, Durham, NC 27705, USA

[2]Department of Medicine, University of North Carolina at Chapel Hill, Chapel Hill, NC 27599 USA

[3]Department of Textile Technology, RWTH Aachen University, Aachen, 52062, Germany

[4]Duke Molecular Physiology Institute, Duke University Medical Center, Durham, NC 27701, USA

[5]Department of Medicine, Duke University Medical Center, Durham, NC 27710, USA

[6]Department of Cardiology, Duke University Medical Center, Durham, NC 27710, USA

Abstract

A number of significant muscle diseases, such as cachexia, sarcopenia, systemic chronic inflammation, along with inflammatory myopathies share TNF-α-dominated inflammation in their pathogenesis. In addition, inflammatory episodes may increase susceptibility to drug toxicity. To assess the effect of TNF-α-induced inflammation on drug responses, we engineered 3D, human skeletal myobundles, chronically exposed them to TNF-α during maturation, and measured the combined response of TNF-α and the chemotherapeutic doxorubicin on muscle function. First, the myobundle inflammatory environment was characterized by assessing the effects of TNF-α on 2D human skeletal muscle cultures and 3D human myobundles. High doses of TNF-α inhibited maturation in human 2D cultures and maturation and function in 3D myobundles. Then, a tetanus force dose-response curve was constructed to characterize doxorubicin's effects on function alone. The combination of TNF-α and 10nM doxorubicin exhibited a synergistic effect on both twitch and tetanus force production. Overall, the results demonstrated that inflammation of a 3D, human skeletal muscle inflammatory system alters the response to doxorubicin.

KEY TERMS

Tissue engineering; human skeletal muscle; inflammation; TNF-α; drug testing; muscle regeneration

*Corresponding Author. T: (919) 660-5147. F: (919) 684-4488, george.truskey@duke.edu, Address: 1395 FCIEMS, 101 Science Drive, Durham, NC 27708-0281.

INTRODUCTION

A number of significant muscle diseases, such as cachexia, sarcopenia, systemic chronic inflammation, along with inflammatory myopathies share inflammation in their pathogenesis[11,34,47]. Inflammation is a necessary response to muscle injury and aids in regeneration. However, inappropriate or unregulated inflammatory reactions may cause tissue injury. An episode of inflammation during drug treatment can predispose animals to tissue injury[5,23]. In addition, inhibition of the production or bioactivity of the proinflammatory cytokine, TNF-α, markedly reduces the toxicity of many drugs in animal models[36]. Taken together, the presence or absence of inflammation characterized by TNF-α may be another susceptibility factor for drug-induced injury.

TNF-α-based inflammatory stress may decrease the threshold for drug toxicity, thereby narrowing the therapeutic window, the range in which the drug is therapeutic but not toxic. For example, a variety of drugs can cause myopathies with weakness and muscle pain even at prescribed doses within the therapeutic window[42]. A plausible hypothesis is that chronic inflammation sensitizes skeletal muscle to drug-induced toxicity. An understanding of the role that TNF-α plays in the pathogenesis of drug-induced muscle disease is important for the development of preventative adjunctive therapies.

To test how well we can model the effect of TNF-α on drug responses, we engineered 3D, human skeletal myobundles and characterized their response to TNF-α *in vitro*[7]. In contrast to 2D cultures, the 3D human skeletal muscle (hSkM) myobundles can produce functional outputs, such as twitch and tetanus contractile forces, that are indicative of overall bundle health. Furthermore, this system enables the examination of TNFα-initiated effects independently and in conjunction with those of other drugs in an orientation mimicking *in vivo* muscle.

The drug candidate chosen to validate our system was doxorubicin. Doxorubicin is one of the most effective and common chemotherapeutics administered to treat cancer; additionally, cancer is commonly associated with elevated cytokine levels[15,34]. Thus, studying the interaction between elevated TNF-α concentrations and drugs with known muscle-weakening effects such as doxorubicin is significant in determining the full extent of drug toxicity in relevant clinical settings[22].

Initially to validate the proposed 3D myobundle model, experiments were performed with the murine C2C12 cell line to determine whether our cell culture protocols replicate the effect of TNF-α on myogenesis commonly reported in the literature (Supplemental Table S1). The effects of TNF-α on maturation were then assessed in the hSkM myobundles consisting of myotubes, fibrinogen, and synthesized extracellular matrix. Using the hSkM tissue-engineered myobundles, we evaluated the functional effects of TNF-α on human muscle maturation by measuring contractile force. We also investigated the mechanism by which differentiation is inhibited through measuring the relationship between maturation and either cell death or NF-κB activation. Lastly, we measured the isolated and combined effects of TNF-α and doxorubicin dosage on muscle weakness. These results serve as evidence that

our model can yield information about the additive effects of toxic drugs and chronic TNF-α presence.

MATERIALS AND METHODS

Primary human myoblast culture

Muscle biopsies were obtained from discarded surgical waste with Duke IRB approved protocols. Human skeletal muscle myoblasts were isolated according to previously described methods[12]. Briefly, muscle samples were minced, washed in phosphate buffered saline (PBS), and enzymatically digested in 0.05% trypsin for 30 minutes. Muscle samples were collected by centrifugation, pre-plated for 2hr, and transferred to a Matrigel (BD Biosciences, San Jose, CA) coated flask for attachment. Myoblasts were cultured in human growth media (hGM) containing low glucose (1 g/L; LG) DMEM (GIBCO/Invitrogen) supplemented with 8% fetal bovine serum (Hyclone), 1x antibiotic-antimycotic, and SkGM SingleQuots (Lonza) without insulin or Gentamicin/Amphotericin-B. Myoblasts were seeded in either 6 or 12-well plates, 60 mm dishes, or engineered myobundles.

Myoblasts were plated and grown to 60% confluency. To induce differentiation, the media was switched to human differentiation media (hDM) was consisting of LG DMEM supplemented with 2% horse serum (HS; Hyclone), 1x antibiotic-antimycotic, and 10nM insulin (Lonza).

C2C12 myoblast culture

The murine C2C12 cell line myoblasts were cultured in C2C12 growth media (C2C12 GM) containing high glucose (HG;4.5g/L D-glucose) DMEM, 8% fetal bovine serum, 8% bovine calf serum (Hyclone), 0.5% chick embryo extract (Accurate Chemical), and 1x antibiotic-antimycotic. Myoblasts were seeded in either 6 or 12-well plates or 60mm dishes.

Myoblasts were cultured in C2C12 GM until reaching 60% confluency then shifted to HG DMEM (GIBCO/Invitrogen) supplemented with 8% HS, and 1x antibiotic-antimycotic to induce myofiber formation and differentiation.

Human and C2C12 TNF-α and doxorubicin dosing in monoculture and myobundles

At the onset of differentiation, either 0.1% BSA (vehicle control) or TNF-α (100–10,000U/mL) was added to the cultures and refreshed daily. Endpoint assays assessing effects of TNF-α were run on day 1 (EdU; C2C12), day 2 (EdU; human), day 3 (quantifying protein, DNA, immunostaining, force production; C2C12) and day 5 of differentiation (quantifying protein, DNA, immunostaining, force production; human). From day 5 to day 12 of differentiation, human cultures were dosed every other day with either 100U/mL TNF-α or 0.1% BSA in combination with either doxorubicin or 0.1% DMSO.

Total cellular protein and DNA quantification

The cells were washed twice with DPBS and detached from the dish using a cell scraper. The cell solutions were split in half for protein isolation and DNA isolation.

Protein was isolated from cells and quantified as described previously[8]. Briefly, cells were harvested with a cell scraper and lysed using CellLytic-M (Sigma) and protease inhibitor cocktail (Sigma). Protein concentration was assessed using the bicinchoninic acid (BCA) protein assay kit (Pierce). Protein samples and BSA standards were added to working reagent, covered, incubated for 30 minutes at 37C, and the absorbance at 562mn was measured. DNA isolation was performed by modifying the Qiagen DNeasy blood & tissue kit standard protocol. Briefly, the cells were harvested with a cell scraper and incubated at 56C in a 10:1:10 mixture of PBS, proteinase K, and Buffer AL for 15 minutes. After the incubation, 200μL of ethanol was added and the mixture was run through the spin column. The sample was washed with 500μL of Buffer AW1, 500μL of Buffer AW2, then was finally eluted with 200μL of Buffer AE. A Nanodrop 1000 spectrophotometer was used to determine DNA concentration (260nm). Calculated protein masses were normalized with DNA mass per dish.

Primary human and C2C12 myoblast proliferation assay

Cellular proliferation was assessed as previously described using an Invitrogen EdU assay[39]. Briefly, cells were washed 3x with DPBS. After incubating for 2hr with EdU, cells were fixed and permeabilized with methanol. The Click-iT reaction cocktail was added as described (Invitrogen). After washing 3x with DPBS, DNA was stained with 4mM Hoechst 33342 in DPBS for 30 minutes then imaged. Results are reported as the fraction of EdU-stained cells to the total number of nuclei present.

Monoculture immunofluorescence

Wells were washed twice with warm DPBS, fixed with ice cold methanol for 5 minutes, washed 3x with DPBS, and then washed 3x with wash buffer (DPBS/0.02% Tween20). After incubating for 1.5hr in blocking solution (10% goat serum in DPBS/0.02% Tween20), cells were incubated with either anti-MHC [MF20 (DSHB);1:50], or anti-nuclear factor kappa B (NF-κB) [Cell Signaling Technologies;1:400]. After washing with wash buffer, secondary antibody (1:250) and Hoechst33342 (1:1000) were added in blocking solution for 2hr at 37°C. Samples were then washed 3x with wash buffer and 3x with DPBS. A Nikon Eclipse TE2000-U inverted microscope was used to capture images.

Imaris 7.0 was used to determine the percent of nuclei in MHC positive cells and NF-κB nuclear translocation. ImageJ was used to measure percent area stained positive for MHC and metrics of muscle cell fusion (myotube diameter, myotube length, and average number of nuclei per myotube). Five randomly chosen micron squares from a larger stitched image were used for analysis, and averages were recorded.

Human tissue-engineered skeletal muscle bundle culture

The myobundle assembly procedure was used as previously described[9,12,29]. Briefly, cells were dissociated in 0.025% trypsin-EDTA to a single cell solution then encapsulated in a fibrinogen (Akron, Boca Raton, FL) and matrigel solution on laser cut Cerex frames within PDMS molds at 7.5×10^5 cells/myobundle. The cell/hydrogel mixture was polymerized for 30min at 37°C then added to media. Human myobundles were cultured in hGM supplemented with 1.5mg/mL aminocaproic acid (ACA) on a rocker (0.33Hz) at 37°C. On

day 4, the media was switched to differentiation medium (hDM) consisting of LG-DMEM supplemented with 2% adult HS, 2mg/mL of ACA, 10nM insulin, and 1x antibiotic-antimycotic and the myobundles were removed from the molds.

Myobundle immunofluorescence

Myobundles were fixed for 5 minutes with ice cold methanol, washed in DPBS, and placed in blocking solution at room temperature for 4hr. Samples were incubated in primary antibodies overnight (anti-MHC,1:50; anti-NF-κB,1:400), washed, then incubated in secondary antibodies and Hoechst dye for 2hr at 37°C. Images were acquired using a Leica SP5 inverted confocal microscope.

Maturation and fusion data analysis

Images were assessed with ImageJ software for fiber diameter, percent of nuclei in fibers and Imaris for NF-κB nuclear translocation. For image analysis, 5 measurements were taken per field of view, 3 fields of view were taken per bundle, and 2–4 myobundles were examined per condition.

Real-time PCR

Total mRNA was isolated using the Aurum total RNA mini kit (Bio-Rad) according to the manufacturer's instructions. mRNA was isolated from 3 myobundles per condition (mRNA yield=3.8±0.4μg/bundle). Quantitative RT-PCR was then used to determine the expression of five different isoforms of MHC using the iTaq Universal SYBR Green One-Step RT-qPCR kit (Bio-Rad) using the manufacturer's recommended protocol. The gene expression was analyzed for type IIX fast (MYH1), embryonic (MYH3), type I slow (MYH7), perinatal (MYH8), and TATA- box binding protein (TBP). Relative quantification of the gene expression was determined using the $\Delta\Delta C_t$ method with TBP as the reference gene.

Contractile function assessment

Force generating capacity of engineered muscle was assessed after 5 days of maturation for the TNF-α studies and 12 days of maturation for the doxorubicin studies. Engineered muscle myobundles were loaded into a custom-made force measurement setup containing a sensitive optical force transducer and a linear actuator (Thor Labs, Newton, NJ) and analyzed as previously described[9,29]. Briefly, one end of the myobundle was secured by a pin to an immobile PDMS block and the other end was attached to a PDMS float connected to the force transducer mounted on a computer-controlled motorized linear actuator. Samples were stimulated (40V/cm) to recreate twitch (1Hz for 10ms) and tetanic (20Hz for 1s) contraction. Contractile force traces were analyzed for peak twitch or tetanus force, time to peak twitch, and half relaxation time.

Force dose response curves were collected by measuring tetanus force of myobundles treated with vehicle or doxorubicin (0.1–750nM). Vehicle tetanus force was set at 100% to which all other points were related. A nonlinear regression model was fit to the data with the equation, $Y=\Phi+(\beta-\Phi)/(1+10\text{^}((\text{Log}(X)-\text{Log}IC_{50})))$, to determine the IC_{50} of doxorubicin, where, Φ is the bottom plateau of the curve, β is the top plateau of the curve, and IC_{50} is the concentration of doxorubicin that inhibits half of tetanus force production.

Two doxorubicin concentrations (1nM and 10nM), and the vehicle control were chosen to characterize the combined influence of doxorubicin and 100U/mL TNF-α on twitch and tetanus force.

Lactate dehydrogenase (LDH) assay

Lactate dehydrogenase was measured every other day during initial culture (days 2 and 4) and after incubations with either 0.1% DMSO (vehicle control), 1nM doxorubicin, or 10nM doxorubicin in hDM (days 7,9,11, and 12). The LDH concentration was quantified using the Pierce LDH cytotoxicity assay kit (Thermo Scientific, Pittsburgh, PA) by following the manufacturer's recommended protocol. The results are presented as the percent of the positive control (lysed myobundle) using the following equation: LDH release = (sample LDH–media control)/(positive control–media control)x100%.

Statistical analysis

The data are presented as mean±SEM. Statistical analyses were carried out using one-way ANOVA, two-way ANOVA, and unpaired t-test as appropriate. A Dunnett post hoc test was used for intergroup comparisons (Graphpad Prism 5, Graphpad Software). The Bliss independence model was used to assess the additive and synergistic effects of the doxorubicin and TNF-α combination on force production. Predicted additive values were calculated using the following equation: $Y_{ab,p}=Y_a+Y_b-Y_a*Y_b$[46]. Where $Y_{ab,p}$ is the predicted fraction of inhibition of force if the two drugs were additive, Y_a is the fraction of inhibition by doxorubicin, Y_b is the fraction of inhibition by TNF-α. Statistical significance is shown as *p<0.05,**p<0.01,#p<0.001.

RESULTS

Effects of TNF-α on protein content and proliferation of 2D C2C12 and hSkM cultures

In C2C12 cultures at day 3 post-differentiation, we assessed myotube protein content, DNA content, and proliferation. The myotube normalized protein content (μg protein/μg DNA) decreased as TNF-α concentration increased, with significant differences observed starting at 1,000U/mL (p<0.01) (Figure 1A). The normalization of protein data was necessary to account for an increased number of cells due to the increase in DNA content with increasing concentrations of TNF-α. Significant differences in DNA content were observed starting at 100U/mL (p<0.001) (Figure 1B). The mechanism behind DNA content increases was probed by measuring the percent of cellular proliferation in a 2-hour period. TNF-α increased the percentage of cellular proliferation in a dose-dependent manner (Figure 1C). These data indicated that the increased DNA per plate was due to TNF-α-induced increased proliferation.

In contrast to C2C12 cultures, TNF-α only decreased hSkM protein content at a concentration of 10,000U/mL (p<0.01); at this high concentration, a 20% protein content reduction was found (Figure 1D). Similarly, the DNA content also increased at 10,000U/mL (p<0.01; Figure 1E). For this sample size, no increased proliferation was measured in TNF-α dosed hSkM cultures (Figure 1F). TNF-α altered hSkM protein and DNA but concentrations were comparatively much higher than those required in C2C12 cultures[27].

Effects of TNF-α on differentiation of 2D C2C12 and hSkM cultures

TNF-α's inhibitory influence on myoblast differentiation was examined using MHC immunofluorescent staining. MHC protein expression is indicative of myotube maturation[43]. MHC protein expression was inhibited with increased TNF-α concentrations for both C2C12 muscle cells on day 3 and human muscle cells on day 5 post-differentiation (Figure 2A–H).

In C2C12 cultures, TNF-α-induced significant decreases ($p<0.001$) in both the percent of total nuclei in MHC positive myotubes (Figure 2I) and percent of MHC positive area in the total image field of view (Figure 2J). Both significant differences started at 100U/mL. At 10,000U/mL, there is an 85% and 73% reduction in percent total nuclei in MHC positive fibers and percent of MHC positive area, respectively. Similarly, for the same metrics, hSkM cultures also trended downward with increasing TNF-α concentrations. HSkM data for individual donors are presented when there is significant variation among donors. To account for donor specific effects, a twoway ANOVA was applied. The interaction between TNF-α concentration and muscle tissue donor was significant ($p<0.05$). With the exclusion of donor 2 at 100U/mL, all TNF-α concentrations yielded decreases in percent total nuclei in MHC myotubes for each donor ($p<0.01$; Figure 2K). Similarly, percent of total area stained for MHC was affected by both TNF-α concentration and donor ($p<0.001$; Figure 2L). Thus, despite noticeable donor-to-donor variability in the magnitude of the response, increasing TNF-α concentration decreased MHC expression.

Furthermore, TNF-α dosed C2C12 and human differentiating myoblasts fused less when compared to those in the control group. Firstly, the C2C12 average number of nuclei per fiber decreased at 100U/mL TNF-α then plateaued at higher concentrations ($p<0.001$;Figure 2M). In contrast, hSkM fusion parameters exhibited higher variability, much like the behavior observed in overall protein content. The number of nuclei per fiber decreased as the TNF-α concentration was increased with a significant difference at 1,000U/mL ($p<0.01$; Figure 2N). While the average number of nuclei per fiber closely resembles those of C2C12 cultures, hSkM fiber dimensions were somewhat larger. This was not unexpected, since hSkM primary cells are larger than C2C12 primary cells; they were also differentiated for a longer time period[8].

In both species, differences in average myotube diameter and length followed these patterns. For C2C12 cultures, myotube diameter and length peaked at 100U/mL. This plateau trend indicates that in C2C12 cultures, fusion was inhibited maximally at 100U/mL TNF-α (Figures 3A, B). Likewise, hSkM myotube diameter and length were reduced maximally at 100U/mL TNF-α also (Figures 3C, D).

Inhibition of myotube fusion in TNF-α treated myobundles

Human myobundle width and myotube fusion were reduced after 5 days of differentiation in the presence of TNF-α (Figure 4). Representative images shown in Supplemental Figure 1A–D display the inhibition of MHC protein expression as TNF-α concentrations increased. TNF-α concentrations at and above 1,000U/mL resulted in reduced myotube diameter (Figure 4A). TNF-α also induced decreases in the number of nuclei per fiber at

supraphysiological concentrations (Figure 4B). Complementing this measure of fusion, percent nuclei in MHC positive fibers significantly decreased in all concentrations above 1,000U/mL TNF-α (Figure 4C). For percent nuclei in MHC positive fibers, the 2D cultures exhibited a higher sensitivity to TNF-α than the myobundles. Similarly, the myobundle cultures exhibited 2 times more fusion; myobundles averaged 8.0±0.4nuclei/fiber, whereas, 2D culture averaged 3.7±0.3nuclei/fiber. This sensitivity difference between 2D and myobundles is not specific to TNF-α; neoplastic cells also have increased drug sensitivity in 2D when compared to 3D and *in vivo* conditions[21]. This suggests that the results from the myobundle constructs are more indicative of the skeletal muscle inflammation environment *in vivo*.

To evaluate if this difference in TNF-α sensitivity could be driven by NF-κB activation, NF-κB translocation was measured in both 2D and myobundle cultures exposed to TNF-α (Supplemental Figure S3). NF-κB activation trends upward with time in a 2D setting but there is no difference after 120hr in myobundles. This mirrors the TNF-α-mediated extent myotube fusion inhibition between the 2D and myobundle cultures suggesting that NF-κB may be driving this inhibitory effect of TNF-α on myogenesis.

To assess whether the inhibitory effect of TNF-α on myogenesis was apparent at the mRNA level, differentiating human myobundles were analyzed for the expression of developmental and adult MHC isoforms (Figure 4D). When treated with TNF-α, MHC isoforms were reduced significantly in all conditions ($p<0.05$). These results illustrate that TNF-α's inhibitory effects on myogenic differentiation are apparent at the gene expression level as well.

TNF-α decreases tetanus contractile force

Myobundle twitch and tetanus forces displayed a downward trend with increasing TNF-α concentration for three different donors (Figure 5A,B). Due to the high variability between donor replicates, only the 10,000U/mL TNF-α twitch force condition was different than the control for two out of three donors ($p<0.05$). Whereas for tetanus force, all donors were different than the control at the highest TNF-α concentration ($p<0.05$). Tetanus force was decreased as well in donor 1 at the 1,000U/mL TNF-α level. This difference in responsiveness was not surprising due to the donor-to-donor variability seen in MHC expression. To assess if there is a correlation between these two measurements, tetanus force was plotted against the percentage of hSkM nuclei in MHC+ fibers (Figure 5C) in the control group and after being exposed to 10,000U/mL TNF-α. A weighted linear regression indicated a statistically significant slope ($0.04<p<0.05$) correlation coefficient of 0.63. This suggests that TNF-α induced changes in MHC expression could predict TNF-α force depression.

Contractile kinetics were also assessed for TNF-α-induced changes. Time to peak twitch was unchanged in all conditions (Figure 5D). In contrast, 1/2 relaxation time was decreased at 10,000U/mL TNF-α ($p<0.001$; Figure 5E). Interestingly, altered myobundle function corresponded to the reduction in nuclei per fiber but was not as responsive to TNF-α as myotube diameter and MHC expression.

We assessed if the force depression was due to cytotoxicity by measuring the release of LDH into the media. In the first 4 days of myobundle differentiation, results showed no difference in LDH release between 1000U/mL TNF-α and control groups. LDH levels were low, between 3–6%, indicating minimal cell cytotoxicity in the presence of both TNF-α and BSA (Figure 5F). This data suggests that the drop in force production was not due to decreased cell viability.

TNF-α enhances doxorubicin-induced depression in contractile force

Doxorubicin decreased myobundle tetanus force production in a dose-dependent manner (Figure 6A). Muscles were incubated for 5 days with a doxorubicin concentration range of 0.1–1000nM, being below maximal plasma concentrations reached in clinical practice[3]. To find the doxorubicin's half-maximal inhibitory concentration (IC_{50}), the experimental dose-response data was fit by a logistic curve (R^2=0.92). The nonlinear regression model equation for the doxorubicin tetanus force data was: tetanus force as a percent of vehicle=100/1+10^((Log[doxorubicin (nM)])-0.997)). The IC_{50} of doxorubicin derived from the fit was 9.93±0.07nM.

The effect of 100U/mL TNF-α and doxorubicin was explored both independently and together on the myobundles. The TNF-α concentration was optimized to fit 2 criteria: 1) produce a difference in force production on day 12 of differentiation when compared to the control, 2) while still producing a large enough force to detect a difference when doxorubicin was added. These criteria were met with 100U/mL TNF-α myobundle treatment refreshed every other day for 12 days. TNF-α and doxorubicin-treated myobundles were assessed for the peak amplitude of twitch and tetanus force (Figure 6B). The depression of twitch and tetanus force at 1 and 10nM doxorubicin concentrations was exacerbated by addition of TNF-α (Figure 6C,D).

The Bliss independence model was used to evaluate synergy of doxorubicin and TNF-α (Figure 7A–D). Combination of the two treatments on twitch and tetanus force production is additive at 1nM doxorubicin concentrations (Figure 7A,C). At the higher doxorubicin concentration, the combination of doxorubicin and TNF-α was significantly more than additive and thus synergistic (Figure 7B,D).

To assess if cytotoxicity explained the depression of force generation, LDH release into the media was measured. For the sample size, there were no observable trends in LDH release for TNF-α dose, doxorubicin dose, or time (Supplemental Figure S2). This suggests that the TNF-α-induced force depression is not due to increased cytotoxicity.

DISCUSSION

The first goal of this work was to create a hSkM myobundle inflammation model using TNF-α and compare the model's responses to that of 2D human and C2C12 models. TNF-α is the cytokine most prominently linked to muscle pathophysiology[35]. Its chronic expression is associated with muscle wasting and loss of muscle function[28,38], in addition to various diseases including sarcopenia, cancer, and heart failure[17,26,47]. While many *in vitro* studies have shown the effects of TNF-α on C2C12 cells, there has been limited scientific evidence

on its effect on hSkM cultures. Therefore, 2D hSkM and C2C12 baseline studies were performed to examine TNF-α's effects on overall protein content, cellular proliferation and prevalence of the late-stage maturation marker MHC. Using these measures, we optimized the TNF-α concentrations to design the 3D myobundle inflammatory model. Although the myobundle platform in this work is a maturation model, it is applicable in mature muscle because injury occurs constantly and repair is ongoing.

Increasing TNF-α concentrations resulted in decreased normalized protein content in both cell types, although hSkM cultures only decreased at 10,000U/mL. This hSkM higher resistance to TNF-α may be due to physiological differences between species, such as receptor subtype expression, resulting in differing myogenic mechanisms[2]. While the TNF-α-induced decreased protein content in hSkM cultures is consistent with relevant results in Table 1, the reduced level of TNF-α sensitivity differs from C2C12 cultures.

In the absence of TNF-α, comparison of the baseline C2C12 culture myotube formation and myotube width have many similarity to what others have reported[4]. Buttadapur et al.[4] also obtained aligned C2C12 myofibers in fibronectin microprinting or micromolded gelatin. Their myogenic index (percent of C2C12 nuclei in sarcomeric α-actinin-positive myotubes) ranged between approximately 0.13–0.38 after one week. This is comparable to the percent of C2C12 nuclei in MHC-positive myotubes was 0.25±0.04%. Similarly, myotube widths are consistent with other C2C12 *in vitro* studies[4]. However, myotube lengths found in Buttadapur et al.[4] are longer than those observed in this study. This suggests that patterning may be advantageous in promoting fusion.

The magnitude of MHC inhibition varied among different individuals which can be attributed to differing genetic and environmental influences on an individual's response to cytokines[6,13,19]. C2C12 cultures do not exhibit the same magnitude of variability because they are more homogeneous and not from different donors. The hSkM model used in these experiments was able to detect differences in MHC expression to varying TNF-α concentrations between different patients. This ability to distinguish TNF-α response differences shows the potential of using this donor-specific inflammation model for developing personalized medicines.

The 2D hSkM MHC protein expression decrease was larger than the observed overall protein content reduction over the same TNF-α range; this increased reduction indicates that this myofibril protein is targeted preferentially compared to other cytoplasmic proteins. Increased myofibrillar protein degradation, which play an important role in contractile force generation, explains the correlation of elevated TNF-α concentrations with muscle weakening and wasting.

As another indicator of muscle cell differentiation, myoblast fusion into multinucleated tubes was quantified by measuring the average number of nuclei per fiber. In addition, measuring average myotube diameter and length further characterized myotube development. Both cell types had roughly the same range of average myotube number of nuclei, although, as noted previously, there was higher variability in the hSkM cultures. hSkM fiber dimensions indicated a correlation between nuclei quantify and fiber size;

diameters and lengths plateau in both metrics by the 1,000U/mL condition, similar to the number of nuclei per fiber. Decreases on myotube dimensions due to TNF-α, further corroborates decreases in total protein content. Overall, while fusion of myotubes in both 2D cultures of C2C12 and human cells was inhibited by TNF-α, it occurred at a more variable rate in hSkM cultures.

It is also worth noting that for both cell types and orientations, the decreases in number of nuclei per fiber was not directly proportional to decreases in myotube diameter and length. Others have reported similar findings with C2C12 cells in monoculture[30]. In 2D, this may be due to the unaligned, randomly branching geometries of the skeletal muscle fibers that introduces variability in size. Such irregular branching is uncharacteristic of *in vivo* muscle cell differentiation. The myotube fusion is increased by a factor of 2 in the 3D myobundles. The myobundles promote differentiation through increased cellular densities[31,40], uniaxial tension for cell alignment[20], and mimicry of tissue stiffness[1] to assist in replicating physiological muscle tissue structure. In 2D it is generally difficult to place myotubes under tension, whereas in the myobundles, the myotubes are cultured under a passive tension resulting from attachment of myobundles to the frames. In myobundles, the difference in proportion of number of nuclei per fiber and fiber diameter might be due to fibers moving in and out of the focal plane. Fibers in multiple focal plans might yield a lower nuclei per fiber count. When the fraction of nuclei in MHC-positive fibers is examined, it is directly proportional to the myotube diameter.

NF-κB links the inhibition of muscle differentiation by TNF-α to the negative regulation of myogenic regulatory factors, especially MyoD[16,25]. TNF-α suppresses MyoD through down-regulation of both gene and protein expression[16,25]. MyoD mRNA are down-regulated at the posttranscriptional level via miRNA[16]. Whereas, MyoD protein abundance is reduced via increased MyoD proteolysis by the ubiquitin proteasome pathway[25]. Myogenic regulator factor suppression by TNF-α inhibits muscle differentiation and fusion.

During maturation, decreases in MYH gene expression are proportional to MHC protein expression decreases. This agreement suggests that TNF-α suppresses MHC through regulation of gene expression. This is strengthened by TNF-α having marginal effects on the MHC content of differentiated myofibers[32].

Similar to the fusion parameter number of nuclei per myotube, only 10,000U/mL TNF-α had an effect on contraction. High TNF-α doses (>25,000U/mL) were also required to decrease contractile force of isolated rodent muscle[45]. In comparison to other force generating myobundles[29], our myobundles were tested on differentiation day 5 instead of day 14. We expected lower contractile forces due to less time for myobundle maturation. The force depression was most likely due to inhibition of myogenesis of the myobundles. This work is the first to show that TNF-α in isolation is capable of significantly reducing human skeletal muscle force generation.

Similar to contractile force, 1/2 relaxation time, decreased at 10,000U/mL TNF-α. Skeletal muscle relaxation after a single twitch or a tetanic contraction is initiated by a reduction in sarcoplasmic Ca^{2+} concentration. However in isolated murine myofibers, baseline calcium

levels and calcium transients during contraction were not altered due to TNF-α even though it decreased tetanic force[37]. Reid *et al.* concluded that TNF-α decreases force by blunting the response of muscle myofilaments to calcium activation[37]. This decreased sensitivity to calcium activation could be a factor in the human myobundle decreased force and contraction kinetics.

To assess how well our platform can model the effect of inflammation on drug responses, we treated the myobundles with both TNF-α and doxorubicin. Doxorubicin is one of the most widely used anticancer drugs for the treatment of carcinoma, sarcoma, and leukemia[33]. Its therapeutic effects are dose limited due to its toxicity in healthy tissue[41]. This is exacerbated by the fact that skeletal muscle plays an active role in the sequestering and metabolism of doxorubicin[14]. Doxorubicin treatment causes significantly reduced skeletal muscle function[18], as noted by a decline in contractile force and rate of force generation[15], and increased muscular fatigue[44]. Skeletal muscle dysfunction is hypothesized to be due to elevated TNF-α levels leading to increased reactive oxygen species[15].

In this study, the doxorubicin concentration range of 0.1–1000nM was below maximal plasma concentrations reached in clinical practice (1200nM)[3]. We found a dose-dependent, inverse relationship between doxorubicin concentration and human, myobundle tetanus force. Similarly, in isolated murine skeletal muscle, doxorubicin's effects on force production are also dose-dependent[44]. The doxorubicin IC50 value for tetanus force is over 25 times less concentrated than the average plasma concentration of doxorubicin over 24 hours in breast cancer patients (257.7±0.8nM)[3]. Even at low doses, doxorubicin had profound detrimental effects on contractile force over 5 days.

Several experimental models suggest that an episode of inflammation during drug treatment predisposes animals to tissue injury[5,10,23]. Doses of bacterial lipopolysaccharide (LPS) induce TNF-α increases in many animal models and although these increases are not toxic themselves they cause increased toxicity when introduced with many pharmaceuticals. Furthermore, inhibition of the production or action of TNF-α markedly reduced the toxicity of many drugs in animal models[36]. This suggests that inflammation characterized by elevated levels of TNF-α may exacerbate the toxicity of drugs. We utilized our human skeletal muscle model to assess the toxicity of doxorubicin alone and in combination with TNF-α. The doxorubicin and TNF-α combined treatment lead to exacerbation of doxorubicin decrement in both twitch and tetanus force production. The combinatory effect of TNF-α at lower doxorubicin concentrations was additive but higher concentrations was synergistic. Our findings suggest that there is an interaction between doxorubicin and TNF-α treatment on human skeletal muscle. This might be due to augmented reactive oxygen species production from both the TNF-α and doxorubicin treatment. Therefore, patient undergoing chemotherapy might be even more susceptible to muscle loss and weakness due to chronic inflammation-induced exacerbations in drug toxicity.

One limitation to this study is the comparison of human primary myoblast to the C2C12 cell line rather than primary murine myoblasts. However, C2C12 myoblasts are most commonly used when assessing the impact of TNF-α on skeletal muscle[24,30]. Addition of C2C12

myoblasts allowed us to compare our work to prior studies evaluating the effects of TNF-α on skeletal muscle.

Overall, we present a robust, myobundle model of inflamed human skeletal muscle that recapitulates the well-characterized effects of TNF-α. To our knowledge, no studies have been performed investigating TNF-α's effects on human muscle differentiation *in vitro*, and thus we were able to probe the influence of TNF-α more accurately than commonly used animal models. Furthermore, the myobundles utilize cells obtained from separate donors and replicate physiological muscle structure and function. The myobundles enable functional measurement of contractile force which is not possible in 2D culture. Thus, compared to 2D cultures or animal models currently used in preclinical settings that are helpful for screening, our human skeletal myobundle inflammation model is better suited for functional measurements that can be related to in vivo values and has the added benefit of donor variability. Because of these advances, the platform acts as a potential research and diagnostic tool for personalized medicines. Additionally, the myobundle system detected that the combination of TNF-α and doxorubicin induced larger decreases in twitch and tetanus force than doxorubicin alone. Therefore, we demonstrated the feasibility of the human myobundle inflammatory system to act as a drug-toxicity testing platform.

Supplementary Material

Refer to Web version on PubMed Central for supplementary material.

ACKNOWLEGEMENTS

We gratefully acknowledge Chris Jackman and Alastair Khodabukus for excellent technical discussions; Megan Kondash for cell isolation; Ringo Yen for project support. This study was supported by NIH grants UH2TR000505, 4UH3TR000505, UG3TR002142, from NCATS and NIAMS to GAT, as well as an NSF Graduate Research Fellowship to BNJD.

REFERENCES

1. Bajaj P, Reddy B Jr., Millet L, et al. Patterning the differentiation of C2C12 skeletal myoblasts. Integrative biology: quantitative biosciences from nano to macro. 3:897–909, 2011. [PubMed: 21842084]
2. Bareja A, Holt JA, Luo G, et al. Human and Mouse Skeletal Muscle Stem Cells: Convergent and Divergent Mechanisms of Myogenesis. PLoS One. 9:2014.
3. Barpe DR, Rosa DD, Froehlich PE. Pharmacokinetic evaluation of doxorubicin plasma levels in normal and overweight patients with breast cancer and simulation of dose adjustment by different indexes of body mass. European Journal of Pharmaceutical Sciences. 41:458–463, 2010. [PubMed: 20688160]
4. Bettadapur A, Suh GC, Geisse NA, et al. Prolonged Culture of Aligned Skeletal Myotubes on Micromolded Gelatin Hydrogels. Scientific Reports. 6:28855, 2016. [PubMed: 27350122]
5. Buchweitz JP, Ganey PE, Bursian SJ, Roth RA. Underlying endotoxemia augments toxic responses to chlorpromazine: is there a relationship to drug idiosyncrasy? The Journal of pharmacology and experimental therapeutics. 300:460–467, 2002. [PubMed: 11805205]
6. Burska A, Boissinot M, Ponchel F. Cytokines as Biomarkers in Rheumatoid Arthritis. Mediators of Inflammation. 2014:24, 2014.
7. Cheng CS, Davis BN, Madden L, Bursac N, Truskey GA. Physiology and metabolism of tissue-engineered skeletal muscle. Experimental biology and medicine (Maywood, N.J.). 239:1203–1214, 2014.

8. Cheng CS, El-Abd Y, Bui K, et al. Conditions that promote primary human skeletal myoblast culture and muscle differentiation in vitro. American journal of physiology. Cell physiology. 306:C385–395, 2014. [PubMed: 24336652]

9. Cheng CS, Ran L, Bursac N, Kraus WE, Truskey GA. Cell Density and Joint microRNA-133a and microRNA-696 Inhibition Enhance Differentiation and Contractile Function of Engineered Human Skeletal Muscle Tissues. Tissue Eng Part A. 22:573–583, 2016. [PubMed: 26891613]

10. Cheng L, You Q, Yin H, Holt M, Franklin C, Ju C. Effect of polyI:C cotreatment on halothane-induced liver injury in mice. Hepatology (Baltimore, Md.). 49:215–226, 2009.

11. Chiang CH, Chuang CH, Liu SL. Transforming growth factor-beta1 and tumor necrosis factor-alpha are associated with clinical severity and airflow limitation of COPD in an additive manner. Lung. 192:95–102, 2014. [PubMed: 24153451]

12. Davis BNJ, Santoso JW, Walker MJ, et al. Human, Tissue-Engineered, Skeletal Muscle Myobundles to Measure Oxygen Uptake and Assess Mitochondrial Toxicity. Tissue Engineering Part C: Methods. 23:189–199, 2017. [PubMed: 28338413]

13. Dibbs Z, Thornby J, White BG, Mann DL. Natural variability of circulating levels of cytokines and cytokine receptors in patients with heart failure: implications for clinical trials. Journal of the American College of Cardiology. 33:1935–1942, 1999. [PubMed: 10362196]

14. Fabris S, MacLean DA. Skeletal Muscle an Active Compartment in the Sequestering and Metabolism of Doxorubicin Chemotherapy. PloS one. 10:e0139070, 2015. [PubMed: 26401619]

15. Gilliam LAA, Clair DK St.. Chemotherapy-Induced Weakness and Fatigue in Skeletal Muscle: The Role of Oxidative Stress. Antioxidants & Redox Signaling. 15:2543–2563, 2011. [PubMed: 21457105]

16. Guttridge DC, Mayo MW, Madrid LV, Wang CY, Baldwin AS Jr. NF-kappaB-induced loss of MyoD messenger RNA: possible role in muscle decay and cachexia. Science (New York, N.Y.). 289:2363–2366, 2000.

17. Hanna JS. Sarcopenia and critical illness: a deadly combination in the elderly. JPEN. Journal of parenteral and enteral nutrition. 39:273–281, 2015. [PubMed: 25591973]

18. Hayward R, Hydock D, Gibson N, Greufe S, Bredahl E, Parry T. Tissue retention of doxorubicin and its effects on cardiac, smooth, and skeletal muscle function. Journal of physiology and biochemistry. 69:177–187, 2013. [PubMed: 22890792]

19. Hegen H, Adrianto I, Lessard CJ, et al. Cytokine profiles show heterogeneity of interferon-β response in multiple sclerosis patients. Neuroimmunology and Neuroinflammation 3:e202, 2016. [PubMed: 26894205]

20. Heher P, Maleiner B, Pruller J, et al. A novel bioreactor for the generation of highly aligned 3D skeletal muscle-like constructs through orientation of fibrin via application of static strain. Acta biomaterialia. 24:251–265, 2015. [PubMed: 26141153]

21. Hongisto V, Jernstrom S, Fey V, et al. High-throughput 3D screening reveals differences in drug sensitivities between culture models of JIMT1 breast cancer cells. PloS one. 8:e77232, 2013. [PubMed: 24194875]

22. Hydock DS, Lien CY, Jensen BT, Schneider CM, Hayward R. Characterization of the effect of in vivo doxorubicin treatment on skeletal muscle function in the rat. Anticancer research. 31:2023–2028, 2011. [PubMed: 21737618]

23. Inoue K, Takano H, Yanagisawa R, et al. Effects of organic chemicals derived from ambient particulate matter on lung inflammation related to lipopolysaccharide. Archives of toxicology. 80:833–838, 2006. [PubMed: 16639588]

24. Langen RC, Schols AM, Kelders MC, Wouters EF, Janssen-Heininger YM. Inflammatory cytokines inhibit myogenic differentiation through activation of nuclear factor-kappaB. FASEB journal: official publication of the Federation of American Societies for Experimental Biology. 15:1169–1180, 2001. [PubMed: 11344085]

25. Langen RC, Van Der Velden JL, Schols AM, Kelders MC, Wouters EF, Janssen-Heininger YM. Tumor necrosis factor-alpha inhibits myogenic differentiation through MyoD protein destabilization. FASEB journal: official publication of the Federation of American Societies for Experimental Biology. 18:227–237, 2004. [PubMed: 14769817]

26. Lebrec H, Ponce R, Preston BD, Iles J, Born TL, Hooper M. Tumor necrosis factor, tumor necrosis factor inhibition, and cancer risk. Current medical research and opinion. 31:557–574, 2015. [PubMed: 25651481]
27. Li YP, Reid MB. NF-kappaB mediates the protein loss induced by TNF-alpha in differentiated skeletal muscle myotubes. American journal of physiology. Regulatory, integrative and comparative physiology. 279:R1165–1170, 2000.
28. Li YP, Reid MB. Effect of tumor necrosis factor-alpha on skeletal muscle metabolism. Current opinion in rheumatology. 13:483–487, 2001. [PubMed: 11698724]
29. Madden L, Juhas M, Kraus WE, Truskey GA, Bursac N. Bioengineered human myobundles mimic clinical responses of skeletal muscle to drugs. eLife. 4:e04885, 2015. [PubMed: 25575180]
30. Magee P, Pearson S, Allen J. The omega-3 fatty acid, eicosapentaenoic acid (EPA), prevents the damaging effects of tumour necrosis factor (TNF)-alpha during murine skeletal muscle cell differentiation. Lipids in health and disease. 7:24, 2008. [PubMed: 18638380]
31. Martin NR, Passey SL, Player DJ, et al. Factors affecting the structure and maturation of human tissue engineered skeletal muscle. Biomaterials. 34:5759–5765, 2013. [PubMed: 23643182]
32. Miller SC, Ito H, Blau HM, Torti FM. Tumor necrosis factor inhibits human myogenesis in vitro. Molecular and cellular biology. 8:2295–2301, 1988. [PubMed: 3405207]
33. Minotti G, Menna P, Salvatorelli E, Cairo G, Gianni L. Anthracyclines: molecular advances and pharmacologic developments in antitumor activity and cardiotoxicity. Pharmacol Rev. 56:185–229, 2004. [PubMed: 15169927]
34. Pawelczak M, Rosenthal J, Milla S, Liu YH, Shah B. Evaluation of the Pro-inflammatory Cytokine Tumor Necrosis Factor-alpha in Adolescents with Polycystic Ovary Syndrome. Journal of pediatric and adolescent gynecology. 27:356–359, 2014. [PubMed: 25256873]
35. Plomgaard P, Penkowa M, Pedersen BK. Fiber type specific expression of TNF-alpha, IL-6 and IL-18 in human skeletal muscles. Exercise immunology review. 11:53–63, 2005. [PubMed: 16385844]
36. Ramesh G, Reeves WB. TNF-alpha mediates chemokine and cytokine expression and renal injury in cisplatin nephrotoxicity. The Journal of clinical investigation. 110:835–842, 2002. [PubMed: 12235115]
37. Reid MB, Lannergren J, Westerblad H. Respiratory and limb muscle weakness induced by tumor necrosis factor-alpha: involvement of muscle myofilaments. American journal of respiratory and critical care medicine. 166:479–484, 2002. [PubMed: 12186824]
38. Reid MB, Li Y-P. Tumor necrosis factor-α and muscle wasting: a cellular perspective. Respiratory Research. 2:269–272, 2001. [PubMed: 11686894]
39. Rhim C, Cheng CS, Kraus WE, Truskey GA. Effect of MicroRNA Modulation on Bioartificial Muscle Function. Tissue Engineering. Part A. 16:3589–3597, 2010. [PubMed: 20670163]
40. Smith AS, Passey S, Greensmith L, Mudera V, Lewis MP. Characterization and optimization of a simple, repeatable system for the long term in vitro culture of aligned myotubes in 3D. Journal of cellular biochemistry. 113:1044–1053, 2012. [PubMed: 22065378]
41. Tacar O, Sriamornsak P, Dass CR. Doxorubicin: an update on anticancer molecular action, toxicity and novel drug delivery systems. Journal of Pharmacy and Pharmacology. 65:157–170, 2013. [PubMed: 23278683]
42. Valiyil R, Christopher-Stine L. Drug-related myopathies of which the clinician should be aware. Current rheumatology reports. 12:213–220, 2010. [PubMed: 20425521]
43. van der Ven PF, Schaart G, Croes HJ, Jap PH, Ginsel LA, Ramaekers FC. Titin aggregates associated with intermediate filaments align along stress fiber-like structures during human skeletal muscle cell differentiation. Journal of cell science. 106 (Pt 3):749–759, 1993. [PubMed: 8308058]
44. van Norren K, van Helvoort A, Argiles JM, et al. Direct effects of doxorubicin on skeletal muscle contribute to fatigue. British journal of cancer. 100:311–314, 2009. [PubMed: 19165199]
45. Wilcox P, Milliken C, Bressler B. High-dose tumor necrosis factor alpha produces an impairment of hamster diaphragm contractility. Attenuation with a prostaglandin inhibitor. American journal of respiratory and critical care medicine. 153:1611–1615, 1996. [PubMed: 8630610]

46. Yang H, Novick SJ, Zhao W. Drug Combination Synergy In: Zhao W, Yang H, eds. Statistical Methods in Drug Combination Studies. Vol 69: CRC Press; 2014.

47. Zhao SP, Zeng LH. Elevated plasma levels of tumor necrosis factor in chronic heart failure with cachexia. International journal of cardiology. 58:257–261, 1997. [PubMed: 9076551]

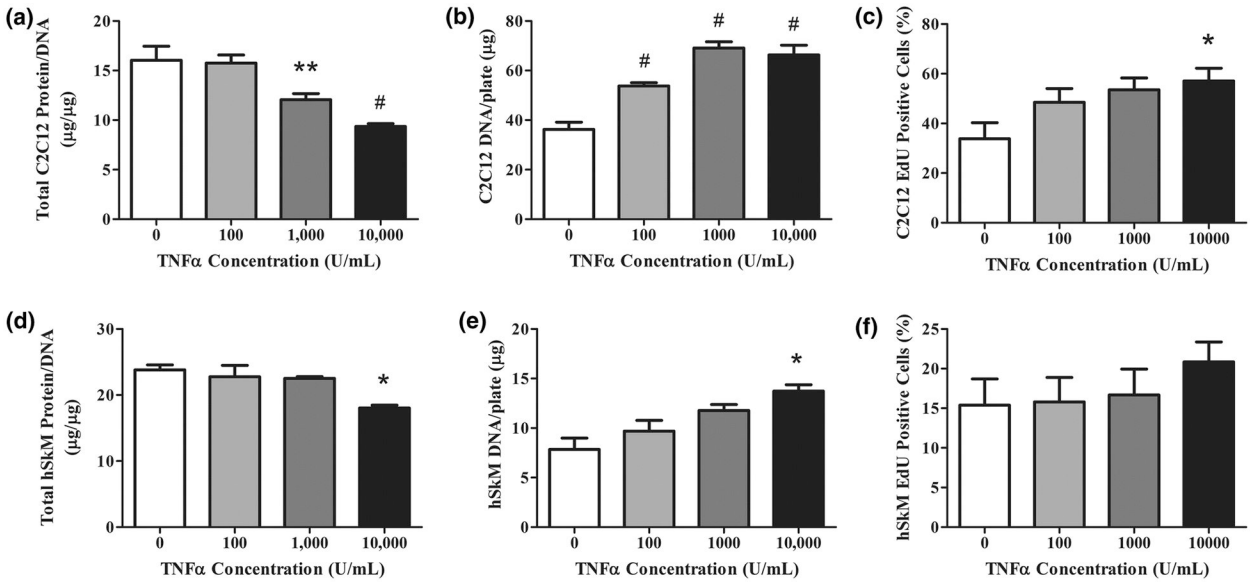

Figure 1.

TNF-α decreases total cellular protein and increases proliferation of differentiating C2C12 and human myoblasts in 2D cultures. TNF-α (0–10,000U/mL) was added daily at the onset of differentiation to (A-C) C2C12 myoblasts for 3 days and (D-F) human myoblasts differentiated for 5 days. A) C2C12 total protein content measured by BCA assay and normalized by mass of DNA for control and TNF-α dose. B) C2C12 DNA mass of myotubes per plate. C) Percent of C2C12 myoblasts proliferating measured by percent of total nuclei staining positive for EdU. Myoblasts were incubated for 2 hours with EdU components after 24 hours of differentiation and TNF-α dosage. D) Normalized protein content and E) DNA mass per plate of hSkM myoblasts on day 3 of differentiation and TNF-α dose. F) Percent of hSkM myoblasts proliferating measured by nuclei staining positive for EdU. Proliferating myoblasts were incubated for 2 hours with EdU components after 24 hours of differentiation and TNF-α dose. Data are mean±SEM for duplicate wells from each of 4 donors. Significance was determined using one-way ANOVA with Bonferroni post-hoc corrections.

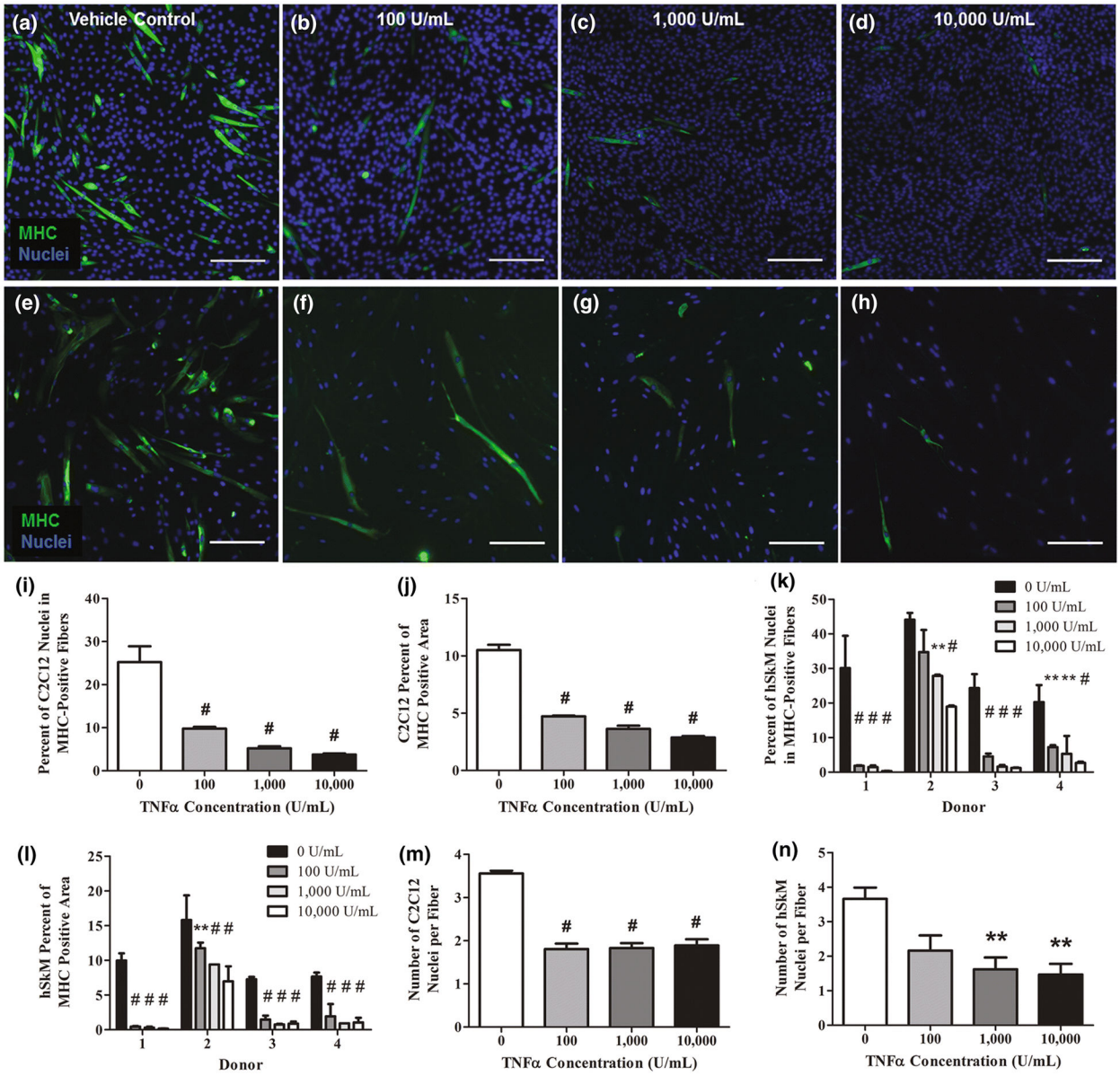

Figure 2.

TNF-α inhibits MHC expression in both C2C12 and human differentiating myoblasts in 2D culture. Immunofluorescent staining for MHC (green) and Hoechst staining for nuclei (blue) revealed the extent of myoblast differentiation at varying concentrations of TNF-α (0-10,000U/mL) after 5 days of daily exposure. There was a noticeable decrease in the expression of MHC in representative images of (A-D) C2C12 differentiating myoblasts cultured with A) vehicle control, B) 100U/mL, C) 1,000U/mL, D) 10,000U/mL of TNF-α. A similar decrease was also seen in representative images of (E-H) hSkM differentiating myoblasts cultured with E) vehicle control, F) 100U/mL, G) 1,000U/mL, H) 10,000U/mL of TNF-α. Scale bar=200μm. The percent of nuclei in MHC-positive fibers and the percent of the total image staining MHC-positive indicated the degree of maturation in differentiating (I,J,M) C2C12 and (K,L,N) hSkM myoblasts after exposure to different TNF-α for 5 days.

All measurements were obtained from immunofluorescent images. I) Percent of C2C12 nuclei in MHC-positive fibers. J) Percent area in the field of view stained positive for MHC in C2C12 cultures. K) Percent of nuclei in MHC-positive fibers in hSkM cultures separated by donor. L) Percent field of view area stained positive for MHC in hSkM cultures separated by donor. M) Number of C2C12 nuclei per fiber. N) Number of hSKM nuclei per fiber. Data are mean±SEM for duplicate wells with 5 fields of view per well from 4 donors for panels I,J,M and N and mean±SEM for duplicate wells with 5 fields of view per well for panels K and L. Significance was determined using one-way or two-way ANOVA with Bonferroni post-hoc corrections.

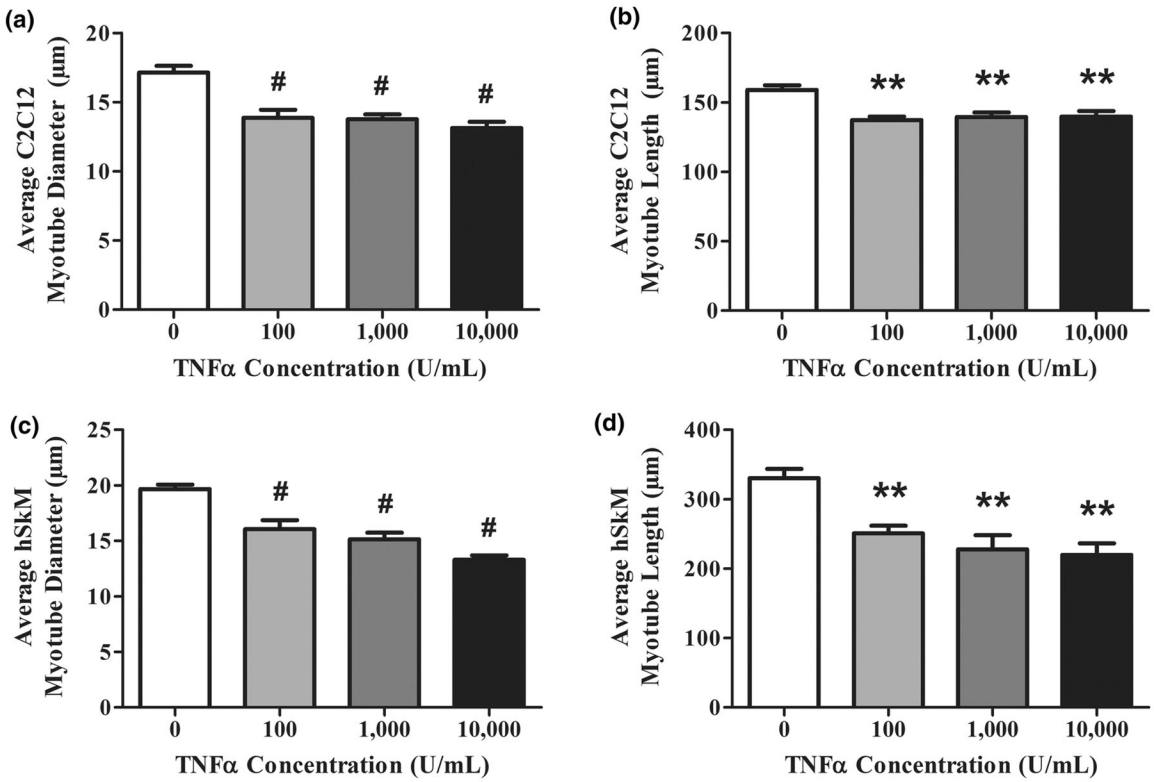

Figure 3.

Myotubes exposed to TNF-α exhibit less fusion in 2D culture. The degree to which myoblasts fuse into multinucleated myotubes is another indicator of skeletal muscle maturation. All (A,B) C2C12 and (C,D) hSkM measurements were obtained by quantifying immunofluorescent images. Data are mean±SEM for duplicate wells from 4 donors. 5 randomly chosen images were analyzed per well. A) Average C2C12 myotube diameter. B) Average C2C12 myotube length. C) Average hSkM myotube diameter. D) Average hSkM myotube length.

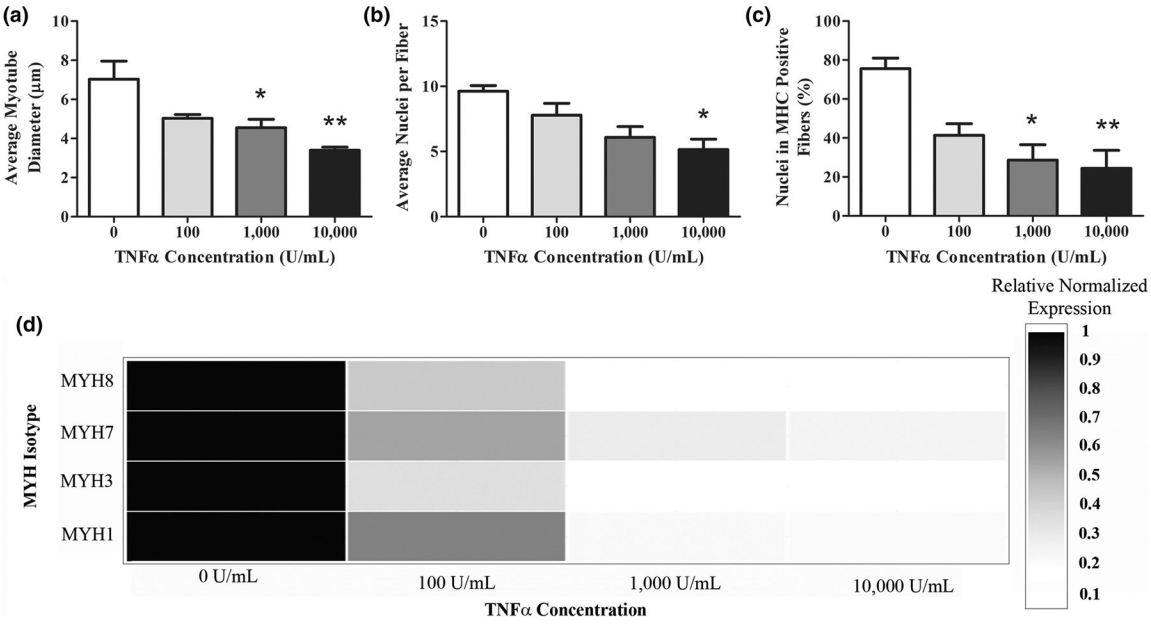

Figure 4.

TNF-α inhibits myogenesis in engineered human myobundles. A-C: analysis of myotube fusion from MHC immunostaining. (A) average myotube diameter, (B) average nuclei per fiber, and (C) percent of nuclei in MHC positive fibers. (D) mRNA expression analysis of myobundles harvested 5 days after daily TNF-α dosing (0–10,000U/mL) started at the onset of differentiation. Genes of interest were the embryonic (MYH3), perinatal (MYH8), and adult MHC isoforms (MYH1, MYH7). Data are expressed as mean for triplicate wells from 3 donors and 2 biological replicates normalized to TBP.

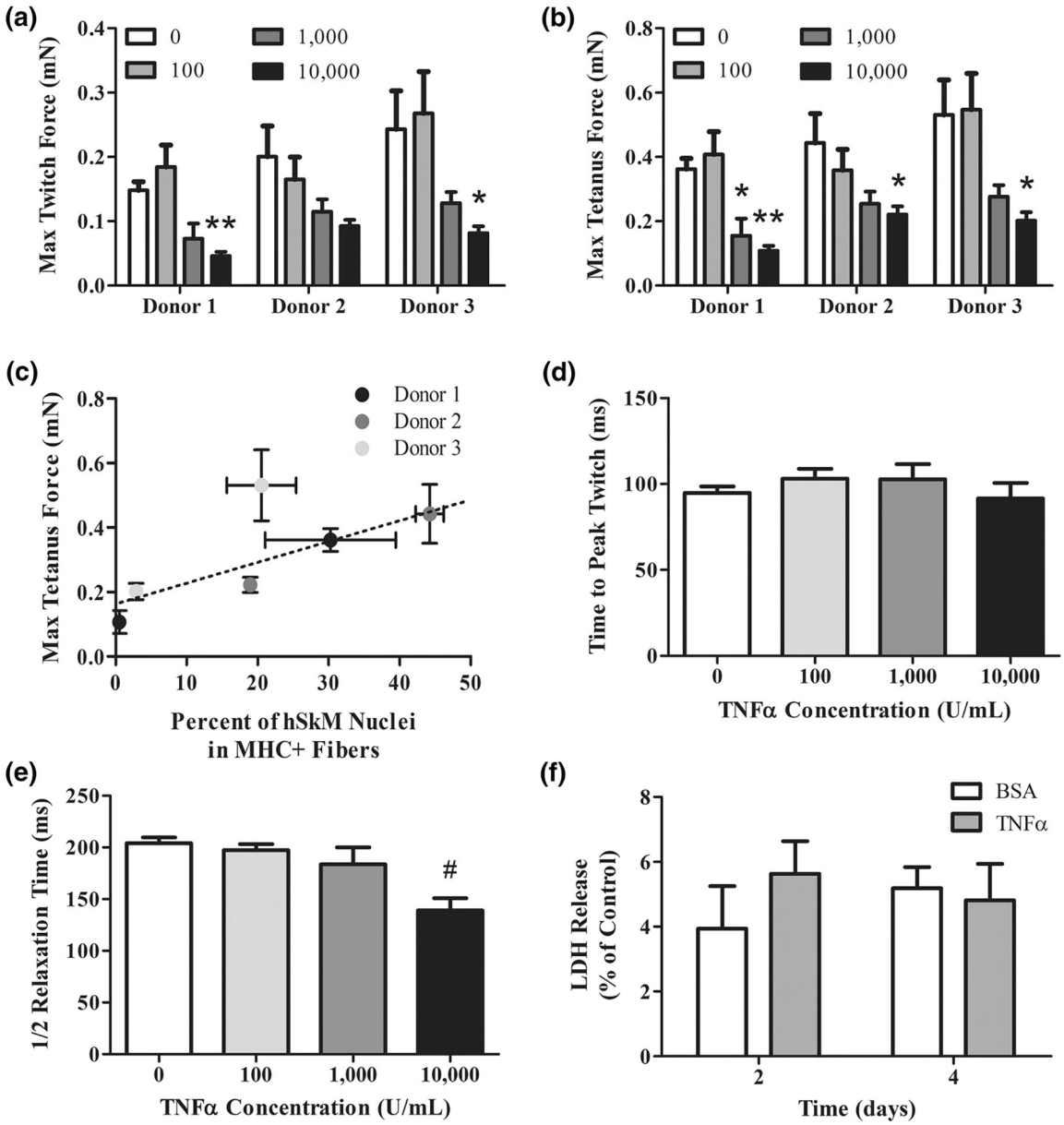

Figure 5.

TNF-α impairs contractile force generation in human myobundles. (A) Myobundles treated daily for 5 days with either vehicle or TNF-α (100–10,000U/mL) at the onset of differentiation displayed an increased depression of both (A) twitch and (B) tetanus force with increasing TNF-α concentrations. (C) Relationship between tetanus force and percent of nuclei in MHC-positive fibers. Data are expressed as mean±SEM of 3 donors with 4 biological replicates. Myobundle (D) time to peak twitch and (E) half relaxation time as a function of TNF-α concentration. (F) Myobundle LDH Release as compared to a lysed control condition after 5 days of daily dosing with 1,000U/mL TNF-α. Data are expressed as mean±SEM of 3 donors with 2 biological replicates per donor.

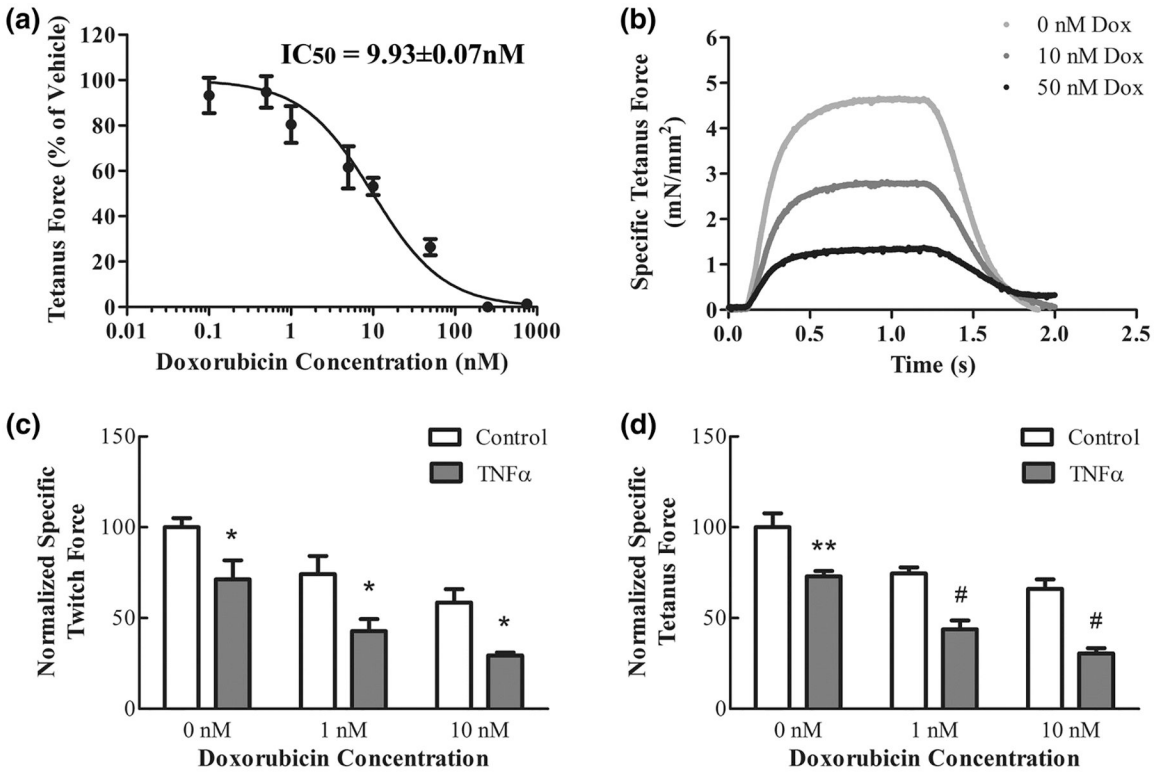

Figure 6.

TNF-α enhances the doxorubicin-induced depression of contractile force in human myobundles. Doxorubicin effects on muscle function were measured by assessing twitch and tetanus force. Myobundles were differentiated for 5 days, then doxorubicin was added every 48 hours for 7 days. (A) Myobundle dose response curve of doxorubicin (0.1–1000nM) for tetanic force depression. (B) Representative vehicle and doxorubicin-treated tetanic force traces. C-D: Myobundles were differentiated for 5 days either in the absence [vehicle (0.1% BSA)] or presence of TNF-α (100U/mL), then doxorubicin was added every 48 hours for 7 days either in the presence or absence of 100U/mL TNF-α. The combination of 100U/mL TNF-α and doxorubicin (1–10nM) had a larger effect on twitch force (C) and (D) tetanus force than doxorubicin alone. Data are expressed as mean±SEM of 4 donors with 4 biological replicates.

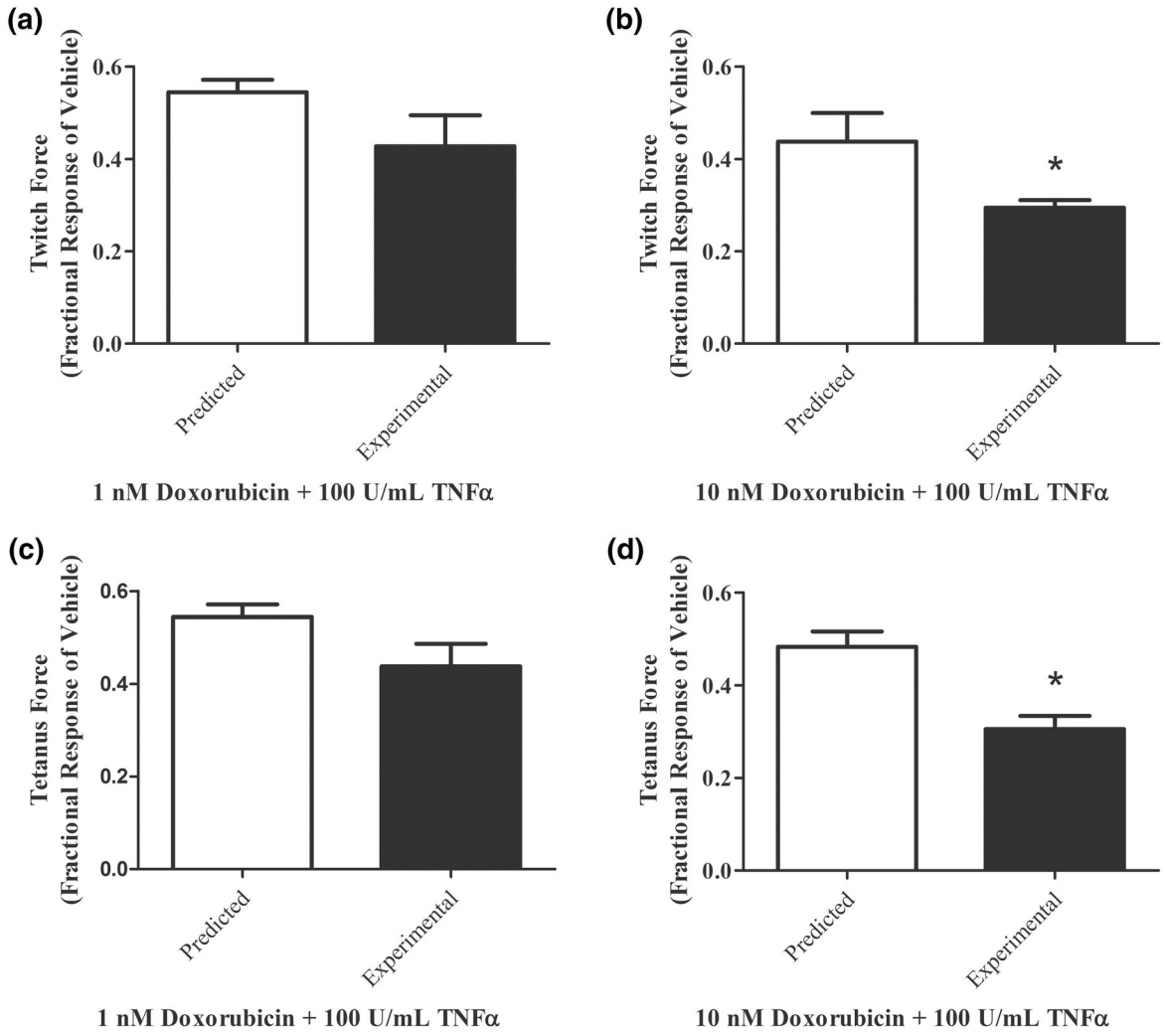

Figure 7.

Doxorubicin contractile depression is exacerbated by 100U/mL TNF-α. (A) Effects of 1nM doxorubicin and TNF-α on twitch force are additive. (B) Effects of 1nM doxorubicin and TNF-α on twitch force are significantly more than additive, thus synergistic. (C) Effects of 10nM doxorubicin and TNF-α on twitch force are additive. (B) Effects of 10nM doxorubicin and TNF-α on twitch force are significantly more than additive, thus synergistic. Data are expressed as mean±SEM of 4 donors with 4 biological replicates.